AMUX-based Bandwidth Tripler with Time-interleaved Nonlinear Digital Pre-distortion Enabling 216-GBd PS-PAM8 Signal

Masanori Nakamura[1], Munehiko Nagatani[1, 2], Hiroshi Yamazaki[1, 2], Teruo Jyo[2], Miwa Mutoh[2], Yuta Shiratori[2], Hitoshi Wakita[2], Hiroki Taniguchi[1], Shuto Yamamoto[1], Fukutaro Hamaoka[1], Takayuki Kobayashi[1], Hiroyuki Takahashi[1, 2], and Yutaka Miyamoto[1]

[1]NTT Network Innovation Laboratories, NTT Corporation, 1-1 Hikarinooka, Yokosuka, Kanagawa, Japan
[2]NTT Device Technology Laboratories, NTT Corporation, 3-1 Morinosato Wakamiya, Atsugi, Kanagawa, Japan
Author e-mail address: msnr.nakamura@ntt.com

Abstract: We propose an analog filterless InP-DHBT AMUX-based bandwidth tripler with a time-interleaved nonlinear digital pre-distortion for tripler and optical frontend impairments, achieving a net-bitrate 496.9-Gb/s signal generation and 483.9-Gb/s 11-km transmission with single-carrier 216-GBd PS-PAM8. © 2024 The Author(s)

1. Introduction

Single-carrier (SC) high-symbol-rate intensity-modulated direct detection (IMDD) systems can enhance capacity while maintaining the number of optical channels and/or parallel fibers, which is effective for next-generation Ethernet for short-reach applications [1]. A 222-GBd on-off keying (OOK) [2] and a faster than Nyquist 570-GBd OOK [3] have been demonstrated for high-symbol-rate IMDD experiments. Moreover, applying a multilevel modulation format to a high-symbol rate signal can increase the capacity. Figure 1 shows the results of the high-speed multilevel 400-Gb/s-class SC-IMDD experiments [1, 4–8]. The bandwidth (BW) limitation of digital-to-analog converters (DACs) in the transmitter is a major obstacle to generating high-symbol-rate multilevel signals. 400-Gb/s-class SC-IMDD experiments have been demonstrated with a high-speed silicon–germanium (SiGe) based time-interleaved (TI)-DAC with an ~80-GHz-BW [1, 4, 5, 8]. A complementary metal-oxide-semiconductor (CMOS) based DAC is widely used for optical transceivers integrated with a digital signal processing (DSP) block. To overcome the BW limitation of a CMOS-based DAC, BW extension techniques have been proposed [6, 7]. A digital pre-processed analog multiplexed DAC (DP-AM-DAC) with an indium phosphide double heterojunction bipolar transistor (InP DHBT)-based analog multiplexer (AMUX) and two channels of CMOS-DACs demonstrated a 400-Gb/s net bitrate of 160-GBd probabilistically shaped (PS)-PAM signals [6]. A digital bandwidth interleaving (DBI), which is composed of a triplexer with a suspended stripline-based analog filter and analog radio frequency (RF) mixers, demonstrated a 494 Gb/s 200-GBd PAM-16 signal multiplexed with three channels of CMOS-DACs [7], and a 226-GBd signal with two channels of SiGe-DACs [9]. Focusing on integration into an optical transmitter, an AMUX-DAC approach including a DP-AM-DAC is attractive due to the analog filterless operation [10]. AMUX-DACs allow flexible signal generation for transmitter-side DSP. Scalability (i.e., the amount of multiplexing) has been, however, limited to two channels of multiplexing (see Fig. 1).

In this paper, we propose an analog filterless AMUX-based BW tripler with a time-interleaved nonlinear digital pre-distortion (TI-NDPD) that compensates for nonlinear imperfection in the tripler, a driver amplifier, and an optical modulator. The tripler multiplexing three channels of CMOS-DACs is composed of a 150-GHz-BW active combiner [11] and >110-GHz-BW AMUXs [12], based on in-house InP DHBT technology. The signal quality improvement of 3.4-dB signal-to-noise ratio (SNR) was obtained with the proposed TI-NDPD. Thanks to the drastic performance improvement by applying the proposed TI-NDPD to the tripler configuration, we achieved 216-GBd PS-PAM-8 SC multilevel signal (see Fig. 1), with a net bitrate of 496.9 Gb/s in back-to-back and 483.9 Gb/s after 11-km transmission.

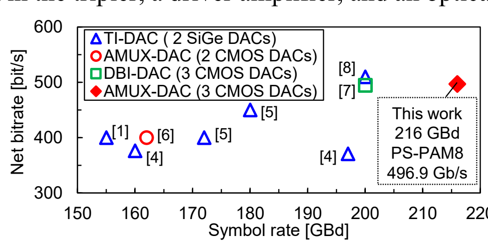

Fig. 1: High-symbol-rate multilevel SC-IMDD experiments with electrical signal multiplexing.

2. Principle

Figure 1 shows a schematic of the BW tripler with Volterra filter (VF)-based TI-NDPD. The tripler consists of two AMUXs and an active combiner. The AMUXs are operated by the clocks with a frequency of $f_{clk} = 2B$, which is one-third of the target symbol rate. The clocks input to the AMUXs have a phase difference of 90 degrees, i.e., these clocks can be expressed as $\cos(2\pi f_{clk} t)$ and $\sin(2\pi f_{clk} t)$. Narrowband signals from DACs with a BW of ~B are

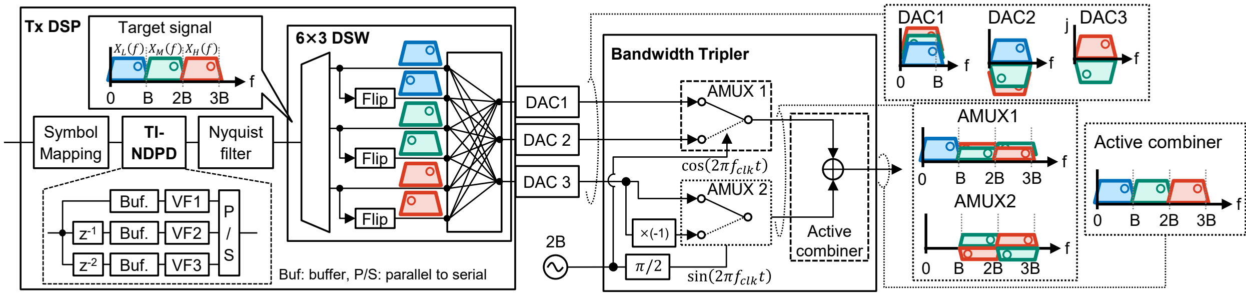

Fig. 2: Schematic of AMUX-based BW tripler DAC with TI-NDPD.

input to the AMUXs, where the signals from DAC1 and DAC2 are input to the AMUX1, and the signal from DAC3 and its inverted signal are input to the AMUX2. The upconverted signals at the AMUXs are combined in an active combiner. In the Tx-DSP, we use a 6×3 digital spectral weaver (DSW) [13] to decompose a wideband target signal to the narrowband signal for the DACs. The DSW also compensates for the linear imperfection in the BW triple with 6×3 multi-input-multi-output (MIMO) equalizer. The six input signals including flipped signals are equalized with appropriate frequency coefficients to the three decomposed signals. For the ideal BW tripler and DACs (without any imperfection), the output decomposed signals from the DSW are as follows: $u_1(t) = \Re\left(\mathcal{F}^{-1}\left[X_L(f) + \frac{1}{2r}\{X_M^*(-f) + X_H(f)\}\right]\right), u_2(t) = \Re\left(\mathcal{F}^{-1}\left[X_L(f) - \frac{1}{2r}\{X_M^*(-f) + X_H(f)\}\right]\right), u_3(t) = \Re\left(\mathcal{F}^{-1}\left[j\frac{1}{2r}\{-X_M^*(-f) + X_H(f)\}\right]\right)$, where $\Re$ is a real part of a complex number, $\mathcal{F}^{-1}(.)$ operates inverse Fourier transformation, r is the amplitude ratio of the tone at f_{clk} to that at dc, and j is an imaginary unit. Then, as shown in Fig. 2, the BW tripler reconstructs the wideband signal expression as $v(kT_s) = u_1(t)\left(1 + r\cos\left(\frac{2\pi}{3}k\right)\right) + u_2(t)\left(1 - r\cos\left(\frac{2\pi}{3}k\right)\right) + u_3(t) r \sin\left(\frac{2\pi}{3}k\right)$, where, k is the symbol index, and T_s is the symbol period of the target signal.

In a practical condition, analog devices including the tripler, a driver amplifier, and an optical modulator cause nonlinear distortion. To improve the signal quality, a conventional VF-based NDPD [6] can compensate for the nonlinearities of the wideband signal. However, a conventional NDPD cannot compensate for the nonlinear distortions for the narrowband signals in the BW tripler because the clocks in the AMUXs affect these narrowband signals. Estimating the nonlinearity for the narrowband signal is also challenging since we can only measure the wideband signal after the BW tripler. To compensate for the nonlinear distortion of both narrowband and wideband signals, we have developed the TI-NDPD shown in Fig. 2. When we consider three symbol index groups of $k = \{3n, 3n + 1, 3n + 2\}$, the effect of the clock on the wideband signal becomes constant for each symbol index group. Therefore, by applying the VF with different coefficients for each symbol index group of the wideband signal, the nonlinear distortion that occurs in the narrowband signal and wideband signal can be simultaneously compensated for. If we set the same coefficients for each VF, the proposed VF-based TI-NDPD is the same as a conventional NDPD. Since the amount of calculation for each VF becomes one-third in the TI-NDPD, the computational complexity of the TI-NDPD to calculate pre-distorted symbols is the same as that of the conventional NDPD.

3. Experimental demonstration

Figure 3 shows the setup for IMDD optical transmission experiments with the proposed BW tripler consisting of the ~150 GHz-BW active combiner [11] and >110 GHz-BW AMUX [12] fabricated by in-house InP DHBT technology. In the Tx-DSP, PS-PAM8 signals with the symbol length of 225,000 were generated from the Mersenne twister. The DSW decomposed the Nyquist shaped PAM8 signal with a roll-off factor of 0.01. A 32-GHz-BW 92.16-GSample/s CMOS-DAC based arbitrary waveform generator (AWG) was used to generate the narrowband signals. The 72-GHz clocks with 90-degree phase differences were generated by using the AWG, a clock quadrupler, and phase shifters.

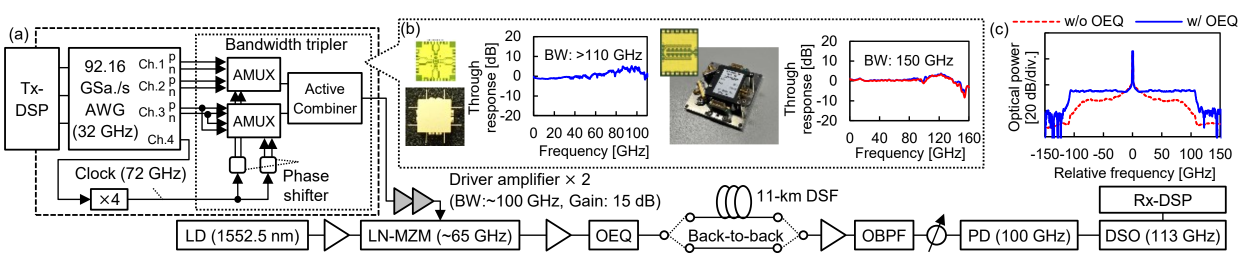

Fig. 3: (a) Experimental setup for 216-GBd PS-PAM8 signal transmission. (b) Through response of AMUX and active combiner. (c) Optical spectra with and without OEQ

The reconstructed wideband signal was amplified in two RF drivers with ~100-GHz-BW and 15-dB-gain in tandem to provide sufficient driving voltage to the ~65-GHz- lithium niobate Mach-Zehnder modulator (LN-MZM). The modulated optical signal at 1552.5 nm was performed by the optical equalization (OEQ) to compensate for the BW limitation of the MZM. To shape the ideal flat-top optical spectrum to avoid noise enhancement at the receiver, the OEQ emphasized ~20 dB at the edge of the spectrum as shown in Fig. 3(c). The optical signals transmitted through 11-km dispersion shift fiber (DSF) with the loss coefficient of ~0.25 dB/km. We used a zero-dispersion wavelength of the DSF. This emulates O-band (1.3-μm) transmission through standard single-mode fiber. The optical signal was received with a ~100-GHz-photodiode (PD) and digitalized in a 113-GHz-BW 256-GSa/s digital storage oscilloscope. In the Rx-DSP, the received signal was equalized with a T/2-spaced 2048-tap feed forward equalizer. Then we calculated the log-likelihood ratios (LLRs) to measure the achievable and net bitrate.

We evaluated the performance of the proposed TI-NDPD, which consists of third-order VFs. Figure 4(a) shows the effective SNR of the 216-GBd uniform PAM8 symbols as a function of the memory length for a conventional third-order NDPD and the proposed TI-NDPD. The coefficients for each VF were determined by least-squares based indirect learning [14] with the symbols for each symbol index group. We used different symbol sequences for estimating the VF coefficients and measuring the SNR to avoid overfitting. The SNRs without NDPD, with the conventional NDPD, and with the proposed TI-NDPD were 11.6, 14.2, and 15.0 dB, respectively. The TI-NDPD obtained an SNR improvement of 3.4 dB from that without nonlinear compensation and an additional gain of 0.8 dB compared with the conventional NDPD. Next, we maximized the net bitrate of the 216-GBd PS-PAM8 signals, which followed a Maxwell-Boltzmann distribution, by optimizing the entropy of symbol probability and the forward error correction (FEC) code rate with an adaptive coding scheme [15]. Figure 4(b) shows the normalized generalized mutual information (NGMI) and the required code rate for each entropy. To determine the required code rate for error-free decoding, LDPC codes defined by DVB-S2 [16] are used with the puncturing method for rate adaptive coding [17] and assumed a 0.9922 code rate outer hard-decision FEC [18]. Figure 4(c) shows the achievable and net bitrate as a function of the entropy of the 216-GBd PS-PAM8 signals. The achievable and net bitrate C are respectively calculated from the NGMI and the code rate R with the equation, $C = [B \cdot \{H - (1 - R) \cdot \log_2 M\}]$, where B is the symbol rate, H is the entropy, M is the modulation order. The maximum achievable and net bitrate were 518.3 Gb/s [=216×(2.82-(1-0.85989)×3)] and 496.9 Gb/s [=216×(2.82-(1-0.82683)×3)] at a back-to-back configuration, respectively. We also conducted 11-km DSF transmission at the zero-dispersion wavelength with the optimized PS-PAM8 entropy. Figure 4(d) shows the received symbol histogram of back-to-back and 11-km transmission. The achievable and net bitrate after 11-km transmission were 512.1 Gb/s [=216×(2.82-(1-0.85038)×3)] and 483.9 Gb/s [=216×(2.82-(1-0.80691)×3)].

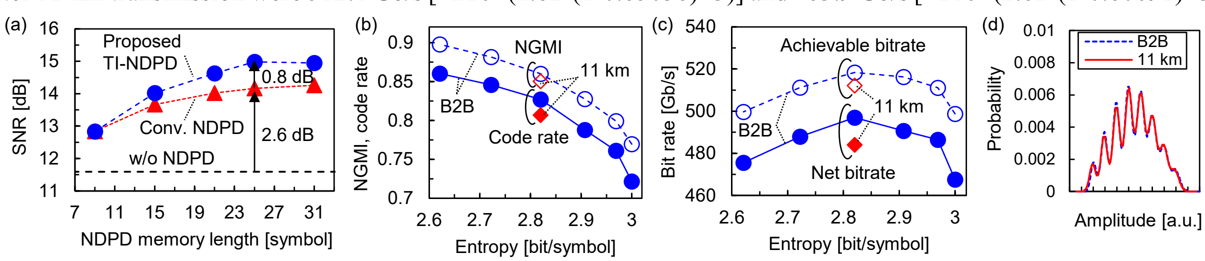

Fig. 4: Experimental results: (a) SNR of Uniform PAM8 vs memory length of third order NDPD, (b) NGMI and code rate vs entropy, (c) achievable and net bitrate vs. entropy of PS-PAM8 signal, and (d) received symbol histogram at back-to-back and after 11-km transmission.

4. Conclusions

We proposed an analog filterless AMUX-base BW tripler with TI-NDPD compensating for nonlinear distortion caused by the tripler and an optical frontend. A high-symbol-rate single-carrier multilevel signal of 216-GBd PS-PAM8 was generated with the proposed BW tripler composed of the 150-GHz BW analog combiner and >110 GHz AMUXs, which multiples three channels of CMOS-DACs. Thanks to the 3.4-dB SNR improvement by using the proposed TI-NDPD, we achieved a net-bitrate 496.9 Gb/s signal generation and 483.9-Gb/s 11-km transmission.

References

[1] H. Taniguchi, et al., in Proc. ECOC2023, Th.B.2.1 (2023).
[2] W. Heni, et al., *J. Lightw. Technol.* 38(9), 2734 (2020).
[3] D. Che, et al., *J. Lightw. Technol*. 40(10), 3347 (2022).
[4] O. Ozolins, et al., in Proc. OFC2023PDP, Th4B.2 (2023).
[5] E. Berikka et al., *Photon. Technol. Lett.*, 35(15), 805 (2023).
[6] H. Yamazaki, et al., *Opt. Exp.*, 27(18), 25544 (2019).
[7] X. Chen, et al., in Proc. ECOC2020PDP, Th3A-2 (2020).
[8] Q. Hu, et al., in Proc. ECOC2023PDP, Th.C.1.7 (2023).
[9] D. Che, et al., in Proc. ECOC2023PDP, Th.C.2.5 (2023).
[10] C. Schmidt et al., *IEEE Commun. Mag.*, 58(5), 19, (2020).
[11] T. Jyo, et al., in Proc. 10b.1, BCICTS 2023 (2023).
[12] M. Nagatani et al., *J. Solid-State Circuits*, 55(9), 2301 (2020).
[13] H. Yamazaki, et al., *J. Lightwave Technol.*, 41(11), 3382 (2023).
[14] P. Berenguer et al., *J. Lightwave Technol.*, 34(8), 1739 (2016).
[15] M. Nakamura, et al., in Proc. ECOC2023PDP, Th3C.1 (2023).
[16] ETSI, DVB-S2; EN 302 307-1, v.1.4.1, (2014).
[17] T. Yoshida, et al., in Proc. OFC2018, M4E.5, (2018).
[18] D. S. Millar, et al., *J. Lightwave Technol.*, 34(6), 1453 (2016).